Available online at www.sciencedirect.com
SCIENCE DIRECT®
Cement & Concrete Composites 27 (2005) 367–379
Cement & Concrete Composites
www.elsevier.com/locate/cemconcomp

Effects of desiccation on mechanical behaviour of concrete

Nicolas Burlion *, Frédéric Bourgeois, Jian-Fu Shao

Laboratory of Mechanics of Lille, UMR CNRS 8107, Polytech'Lille, Cité Scientifique, 59650 Villeneuve d'Ascq, France

Received 29 July 2002; accepted 13 May 2004

Abstract

The objective of this work is experimental characterisation and numerical modelling of coupled behaviours between drying shrinkage and plastic damage in concrete. In the first part, we present an original experimental study on an ordinary concrete in order to determine material damage induced by drying shrinkage. Uniaxial compression tests are performed on samples dried for different periods. It is shown that material damage can be caused by drying process. Mechanical behaviour becomes more brittle with higher damage kinetics when concrete is dried. In the second part, a constitutive model is proposed in order to describe coupled hydro-mechanical behaviour of partially saturated concrete. This model takes into account induced damage, mechanical and capillary plastic deformations. Numerical simulations of experimental tests are presented, and show a qualitatively good agreement with experimental data. The results are relevant with respect to the importance of drying process in the durability study of concrete structures.

Keywords: Concrete; Drying shrinkage; Hydro-mechanical coupling; Damage; Unsaturated material; Elasto-plastic damage model

1. Introduction

One major preoccupations in civil engineering concerns the long-term behaviour of concrete structures, which is the background of a reliable durability analysis. Many concrete structures are subjected to coupled actions of mechanical loading, drying and wetting processes, temperature variation and chemical attack. That makes it very complex to perform a reliable numerical modelling. The purpose of this work is to deal with one important feature of coupled behaviours: effects of drying process on mechanical behaviour of concrete. Indeed, in spite of many studies on the estimation of shrinkage deformation of concrete (see [1–4] for comprehensive synthesis), there are few results concerning effects of drying shrinkage on mechanical behaviour of concrete [1,2,5–7]. Drying shrinkage induces time dependent strains, which can significantly modify stress distribution in many structures. The time dependent induced damage due to drying shrinkage affects the durability of many structures. So far, influences of drying shrinkage on mechanical behaviours of concrete and failure conditions are not properly taken into account in many computer codes, probably due to inadequate knowledge of the associated degradation processes of concrete [1,5].

This paper is composed of two parts. In the first part, some new experimental results are presented. The main purpose of laboratory investigation is to show how basic mechanical behaviour of ordinary concrete is affected by drying shrinkage. In particular, we will study the deterioration of elastic properties of concrete, due to normal drying process, and the dependency of damage process and failure stresses on moisture content. To do this, a new testing programme is proposed. Evolution of drying shrinkage is first measured. Then, uniaxial compression tests are performed on samples submitted to different

* Corresponding author. Fax: +33 3 28 76 73 01.
E-mail address: nicolas.burlion@polytech-lille.fr (N. Burlion).

0958-9465/$ - see front matter © 2004 Elsevier Ltd. All rights reserved.
doi:10.1016/j.cemconcomp.2004.05.004

drying times, and interpreted in terms of elastic properties degradation, failure stresses and plastic deformation. The second part is devoted to constitutive modelling of main behaviours obtained in experimental studies. This is done in the framework of hydro-mechanical modelling of concrete in partially saturated conditions. As the induced damage and plastic deformation represent the common features for most concrete like materials, we propose to use an elasto-plastic damage model. The damage of material is characterised by an extension of the damage model proposed by Mazars [8]. We consider two different mechanisms of plastic deformation, respectively related to mechanical loading and suction variation. Simulations of laboratory tests are provided to show the overall quality of numerical predictions.

2. Experimental investigation

This part presents a comprehensive analysis and some new experimental results for drying shrinkage of concrete. The main purpose is to show the evolution of mechanical properties and induced damage in concrete due to desiccation and drying shrinkage.

2.1. Desiccation of concrete and effects of drying shrinkage on mechanical behaviour

The total shrinkage of concrete is generally decomposed of several parts [1,6,9–11]: autogenous shrinkage including Le Châtelier contraction and self-desiccation shrinkage, thermal shrinkage, carbonation shrinkage and drying shrinkage. The influence of each part is related to concrete composition [2,12–14] and environmental conditions. In this study, only the effects of drying shrinkage are studied. Recently, it was experimentally shown that an important part of microcracking induced by drying is due to, on one hand, the heterogeneous moisture content in the material which induces gradients of drying shrinkage of the cement paste; on the other hand, the heterogeneity induced by the presence of aggregates [15–17].

At macroscopic level, desiccation of concrete is a complex phenomenon. Several types of transfer occur, in two different forms: liquid and vapour. Three types of moisture transport exist [18]: Darcy flow of liquid water, Darcy flow of vapour, and diffusive transfer of vapour. Considering the experimental results that allowed Baroghel-Bouny [12] to identify sorption–desorption isotherm of cylindrical bars, Mainguy et al. [18] analysed the influence of the three kinds of transport on mass loss kinetics of concrete. He showed that for vapour, the Darcy movements are negligible compared to diffusive movements and that diffusive transfer of vapour is small. From the study of vapour molar fraction curves, and after having verified that there was gas overpressures inside the pores, he concluded that rapid uniformity of the vapour molar fraction is achieved. As a consequence, the diffusive transfer of vapour is considerably reduced. A description of water transfers in liquid form with evaporation from the faces of the structure, and the use of a non-linear diffusion equation expressed as a function of degree of saturation or water content, are sufficient to describe correctly the kinetics of concrete mass loss with time [18].

Consequently, the drying shrinkage is caused by drying process through loss of water from concrete. The concrete drying yields local compressive deformation of skeleton material. However, this deformation is partially constrained either by coarse aggregates (local effect) and heterogeneous distribution of moisture state in concrete body (structural effect—i.e. differential shrinkages between the surface and the center of sample). Local tensile stresses may appear and induce initiation and propagation of microcracks [2,15,19]. Shrinkage associated with oven-drying seems to have more damaging effect on the concrete microstructure than compression loading to its maximum capacity [19]. Furthermore, microcracks will change the material elastic properties. The objectives of the current experimental investigation are to show such an effect.

2.2. Concrete composition and testing procedure

Composition of the tested concrete was determined in order to maximise drying shrinkage in a relatively short time. There is a relationship between drying shrinkage and the water by cement ratio (W/C) [13,20]. In general, drying shrinkage increases with the value of this ratio. Indeed, cementitious material with elevated W/C presents a high permeability, facilitating leak-off of water from sample. In addition, more important drying shrinkage would be observed when the maximum size of aggregates is relatively small. Consequently, we have used a concrete with 8 mm maximum aggregate size and a W/C ratio of 0.63. The cement used is of CEM II/B-M (LL-S) 32.5 R CP2 (in European norm EN 197-1). The composition of the concrete is shown in Table 1. With such a W/C ratio, it is expected that the cement matrix will contain large pores [5,12,13] and then present a relatively high drying kinetics. After the curing of 28 days, the porous structure of cement matrix is assumed to be

Table 1
Concrete composition

Cement	324 kg/m^3
Water	205 kg/m^3
Gravel 4/8 mm	1110 kg/m^3
Sand 0/4 mm	668 kg/m^3
W/C ratio	0.63

definitively formed [9], this lets us to consider that moisture diffusion will occur with nearly the same porosity for all specimens.

The structural effect is also an important feature in the study of shrinkage of concrete [2,21,22]. Indeed, the space distribution of moisture is dependent on sample size. The bigger the sample size, the slower is the moisture movement. Inversely, there is a rapid variation of water content in structures with small characteristic size. Accordingly, the effect of drying shrinkage on mechanical behaviour of concrete may be more easily detectable in small size samples [1,22]. However, the size of specimens for mechanical testing should be large enough to preserve the pertinence of representative volume element. In this study, prismatic and cylinder samples are chosen respectively for shrinkage measurement and conventional uniaxial compression tests. The suitable size for cylinder samples is 110 mm diameter and 220 mm height, and the size of prismatic specimens is of $40 \times 40 \times 160$ mm^3.

According to previous works [1,12,13], it is reasonable to assume that autogenous and thermal shrinkage become negligible after 28 days curing, with respect to drying shrinkage for this class of concrete. All specimens were cured in water under a constant temperature of 20 °C for 28 days (Fig. 1). In order to avoid dissolution of portlandite in water, the cylinder samples were simply stored inside their cardboard mould; while prismatic specimens were conserved inside plastic bags immerged in water (Fig. 1). A better way to avoid portlandite dissolution would be to cure sample in water saturated by lime. In our case, for the sake of simplicity, we preferred to directly put samples in thermo-controlled water, by avoiding portlandite exchange by leaving them in their moulds. After 28 days of curing, the specimens were taken out of the water and stored under relative humidity of 60% ± 5% and temperature of 21 °C ± 1 °C (Fig. 1).

We assume that there is an asymptotic stabilisation of drying shrinkage after 90 days according to the concrete composition (W/C = 0.63) [13,22], and the size of prisms ($40 \times 40 \times 160$ mm^3). On the other hand, for cylinders ($\phi = 110$ mm, $h = 220$ mm), the bigger geometry requires longer time to have complete drying [1]. However, the essential part of water mass loss is obtained after 90 days of drying. This lets us to consider that the main shrinkage is produced during this period, which is a reasonable duration for the proposed study. Certainly, quantitative comparison of shrinkage evolution cannot be done due to difference in geometry between the prisms and cylinders, but phenomena should be similar in both cases. The general testing procedure is defined as follows:

- continuous measuring of axial shrinkage deformation of prismatic specimens for 80 days (length variation along the central line of sample),
- regular measuring of weight of prismatic specimens for 80 days,
- regular measuring of weight of cylinder specimens for 80 days,
- uniaxial compression tests with unloading–reloading cycles on cylinder specimens at selected instances, during the 80 days of drying.

2.3. Drying shrinkage results

It is assumed that samples were saturated when they were taken out of the water bath. The global water content is then deduced from the total mass variation of sample. Fig. 2a and b show respectively the evolution of axial shrinkage strain in three prismatic specimens as a function of the time of drying and as a function of loss in mass. These results are similar to those obtained by Granger et al. [21]. In Fig. 2b, two phases can be distinguished. The first part of the curves corresponds to the rapid drying of sample surfaces. This is accompanied by superficial microcracking which delays progress of global shrinkage. Such a behaviour can be attributed to leak-off of free water, which does not induce shrinkage [23,24]. However, many test performed on small size samples have shown a linear relation

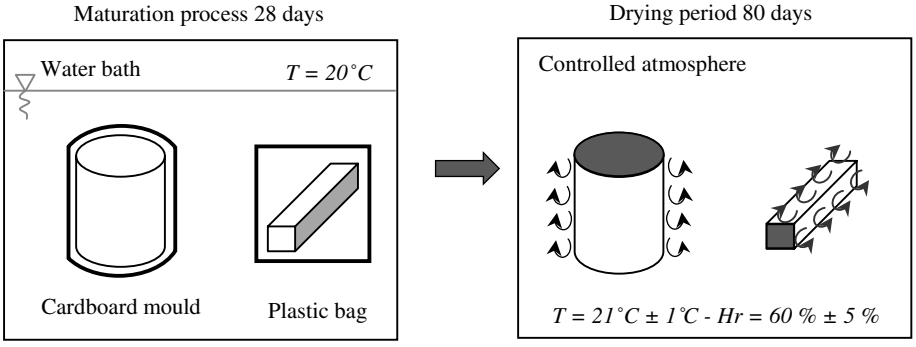

Fig. 1. Conservation conditions of the samples.

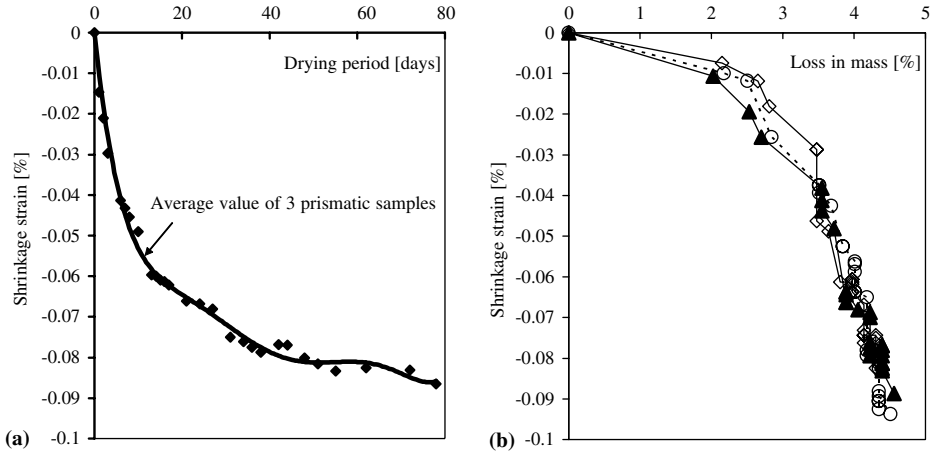

Fig. 2. Evolution of dessiccation shrinkage strain versus time of drying (a) and loss in mass (b) for three prismatic specimens.

between shrinkage and loss of water mass, which is in contradiction with this hypothesis. Granger et al. [21] suggest that this kind of behaviour is rather related to sample surface cracks, which can hide effect of intrinsic drying shrinkage. In the second phase, there is proportionality between loss in mass and shrinkage strain. Microcracks do not evolve at this stage because the moisture gradient tends to vanish. The shrinkage becomes proportional to loss of water mass, like that observed in small size samples. If the measurement was continued after 80 days, a third phase would be obtained where the shrinkage strain would tend to stabilise while the loss in mass continues to evolve [21]. The third phase shows a weight loss evolution without additional drying shrinkage. This last phase can be explained either by the fact that contraction of cement matrix becomes low due to lack of water, by a non-linear drying and drying shrinkage relation, or by a non-linear mechanical behaviour of mortar [25].

Fig. 3 gives the relative variations of total mass of six cylinder specimens (named by their identification numbers G2.8 to G2.59) as functions of drying time. The relative mass is defined as the ratio between the current mass and the initial mass of sample (at 28 days of maturation) before drying. The overall profile is in accordance with classic results reported in literature. However, it is interesting to notice that each specimen considered here was subjected to uniaxial compression test until failure at a selected time (say at 7, 21, 41, 56, 66 and 69 days of drying). After the mechanical test, the specimen was carefully conserved in order to pursue the measurement of weight variation. Comparisons between six samples do not show any correlation between the mass variation rate and the time of performance of mechanical test. This seems to indicate that the influence of mechanical loading on drying kinetics is relatively small, and that the drying process is rather controlled by diffused microcracks than by macroscopic

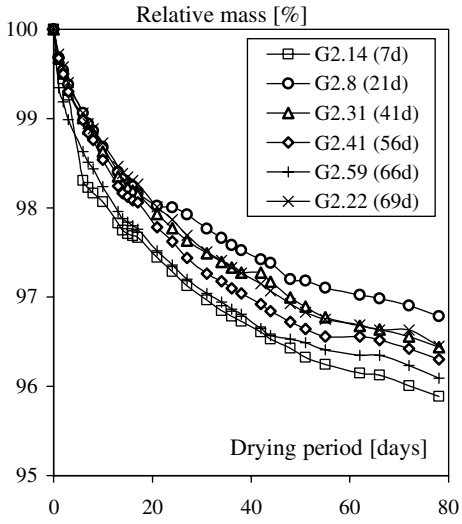

Fig. 3. Evolution of the relative mass during desiccation for six cylindrical specimens tested at different time of drying.

cracks formed under mechanical loading. Notice that the mechanical tests were stopped before complete failure of samples. In uniaxial compression test, only very few (1 or 2) of macro cracks are formed at failure of the sample. This does not significantly increase exchange surface of sample for drying process. According to Bažant et al. [26], cracks in concrete can affect water migration process only if their opening exceeds some millimeters. Therefore, it is not surprising that cracks induced by mechanical loading do not significantly increase velocity of drying process. Further, Meziani and Skoczylas [27] have shown that concrete permeability increases significantly only if the load approaches to failure stress, and it comes to initial value once sample is unloaded. In our study, samples are completely unloaded before continuing drying; this leads to a drying kinetics which is quasi independent of mechanical loading.

2.4. Uniaxial compression tests

Uniaxial compressions were carried out on cylinder samples dried for different durations. All tests were performed under displacement-controlled conditions with a strain rate of $2 \times 10^{-4}\ s^{-1}$ by using a hydraulic machine. The lower platen of the machine is rigid while the upper platen is of kneecap connection. Unloading-reloading cycles were performed at different values of axial stress to determine variation of elastic modulus. It is important to point out that during the drying, water content is not uniform in the test sample, which is a heterogeneous medium. Therefore, overall values of stress, strain and elastic stiffness of the specimen should be used instead of local fields. A typical axial stress versus strain curve obtained in uniaxial compression is presented in Fig. 4. In order to illustrate the influence of drying process on deterioration of concrete elastic properties under mechanical loading, a scalar damage index is defined as the ratio of current elastic modulus (E_i) to the initial elastic modulus (E_0) (as illustrated in Fig. 4). This damage index is defined for every specimen in order to be able to compare its evolution according to the microcracking induced by the drying. The elastic modulus at each cycle is determined from the initial tangent of the reloading curve. However, to avoid unstable responses of samples at the beginning of test, the initial elastic stiffness is determined from the third unloading-reloading cycle in each test (the corresponding nominal axial stress is 9 MPa). The evolution of damage is expressed as a function of the normalised irreversible strain (also named "normalised plastic strain"), which is defined as the irreversible axial strain of each cycle divided by the axial strain at the peak stress of each test. Results obtained from 4 cylinder samples tested respectively at 2, 24, 44 and 69 days are shown in Fig. 5: the notation "G237" is the identification number of sample, and the number "77" is the average water saturation degree

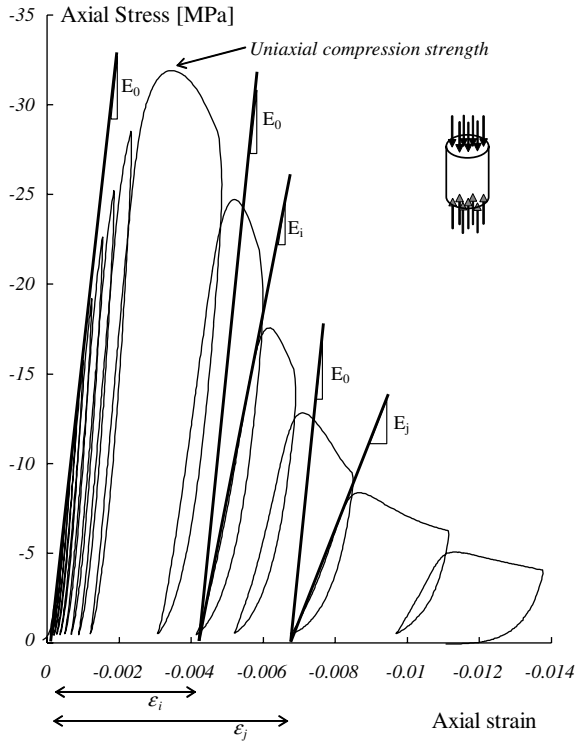

Fig. 4. Typical overall axial stress–strain curve with unloading cycles: definition of elastic stiffness and irreversible strains.

of the sample at the time of mechanical testing; this average saturation degree is estimated from the known loss in mass of the sample and its initial water content (function of its porosity). The water saturation degree after 2 days of drying is still close to 100%. Samples tested after 24, 44 and 69 days of drying have respectively an average saturation degree of about 77%, 68% and 60%. This average saturation degree gives a global indication of drying state as well as the saturation degree is not uniform in samples. It is obvious that there is higher evolution kinetics of damage in specimens dried

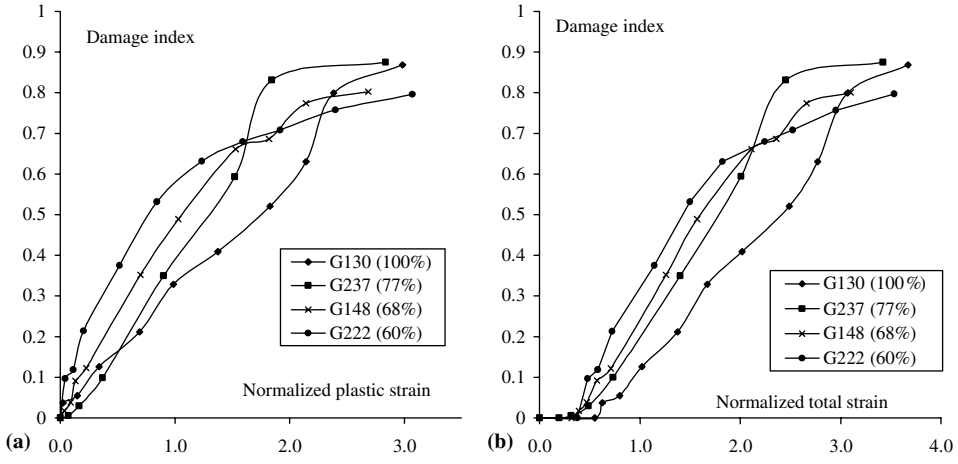

Fig. 5. Evolution of damage versus normalised irreversible strain (a) and normalised total strain (b) for specimens tested at different drying time.

for a longer time. Therefore, the mechanical behaviour of dried concrete becomes more brittle in nature. Propagation of cracks induced by mechanical loading is easier due to initial microcracking which is a consequence of desiccation and drying shrinkage. In Fig. 5a and b, curves are crossing each other. This crossing point occurs for very high damage index (superior to 0.65) corresponding to very large axial strain of the sample: a structural effect appears and damage index have to be carefully analysed. Nevertheless, for smaller damage index, differences between each curve are more pronounced and clearly indicate effects of the microcracks induced by the drying process, which is imposed on the samples before mechanical loading.

Another effect of drying on concrete behaviour is the increase of uniaxial compression strength due to desiccation. This is shown in Fig. 6a and b where one can observe a continuous increase of strength with time of drying (Fig. 6a) or with the loss in mass (Fig. 6b). Each point represent in average 2 tests performed on the same day (so two points on the same day mean that 4 tests were performed). Such a strength increase is usually shown on mortar and concrete, and considered as a consequence of both developed capillary forces and increased surface tension during drying [28–33]. In our modelling, we chose to take into account strength increasing as a consequence of capillary forces (see Section 3). Furthermore, the increase of concrete strength is assumed to come from two concomitant phenomena. The first is capillary suction effect leading to an almost isotropic compression of solid skeleton. As a result, material behaves like a prestressed concrete of higher strength. The second phenomenon is linked to hydrous gradients which are taking place and involving a contraction of the external part of the sample as well as a confinement of sample inside body [1,30]. This "confining lateral pressure" will then induce an increase of strength in the perpendicular direction: the sample is self-reinforced. In addition, water saturated sample of low permeability will bring about interstitial fluid pressure increase. Locally, and by coupling effect, this interstitial overpressure may have an amplifying effect on the propagation and opening of microcracks due to the mechanical axial load [29]. It seems that this strength increase is largely reported by many authors: as an example, Dantec and Terme [34] observed an increase of uniaxial compression strength of 22% at 60% of relative humidity (H_r). Okajima et al. [35] also obtained a progressive increase of compressive strength (about 38%) with the decrease of the relative humidity from 100% to 0%, in the case of a mortar with a W/C ratio of 0.65. Brooks and Neville [36] have measured, at 28, 56 and 84 days, the compressive strengths of concrete samples (W/C = 0.5) cured in water during 28 days, then kept either in water, or in an atmosphere with H_r = 60%: they mentioned that the compressive strengths of dried specimens are always superior to those measured on samples preserved in water. The ratio between the strength measured at 56 days and the one measured at 28 days is equal to 1.1 for saturated specimens, and equal to 1.34 for samples subjected to air drying. Let us note that the mechanical strength decreases between 56 and 84 days, translating the role of the microcracking induced by the drying process on the mechanical damage. Accordingly, Pihlajavaara [28] and Torrenti [37] found respectively a strength decrease of 6% for a mortar and 11% for a concrete between 100% and 50% of H_r. These strength decreases are probably due to the drying induced microcracking which becomes dominant in the failure process, in the case of the cementitious materials used by these authors.

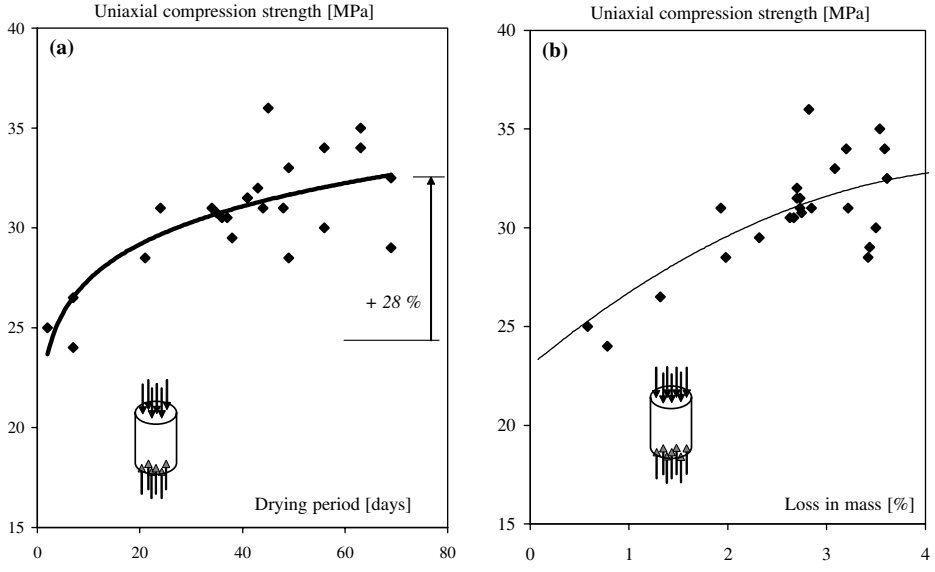

Fig. 6. Evolution of uniaxial compression strength versus drying time (a) and loss in mass (b) from cylinder samples.

It appears necessary to have a series of control samples to validate this assumption. To do this, we have recently conducted a large experimental campaign in our laboratory in order to confirm the increase of mechanical strength due to drying. Mortar samples were conserved in water for 6 months in order to have a complete curing. Samples were then separated into two groups: the first was submitted to drying ($T = 21$ °C, $H_r = 45\%$) and the second is conserved without drying and used as control specimens. No change of mechanical strength was obtained in control samples, while there was an increase of 21% in uniaxial compression strength in dried samples [38]. Moreover, the high W/C ratio used in our concrete (0.63) allows to consider that the hydration is essentially completed during the curing phase. There is a very small increase of strength due to complementary hydration after 28 days in water, compared with the increase of 28% in strength after 70 days of drying. The variability on drying-induced increase of mechanical strength, observed in literature and in the present work, is probably due to different kinds of cement used, differences in gravels (size and granularity) which play a role in matrix-aggregate interface and then on failure stress. Moreover, Baroghel-Bouny et al. have shown that the porous structure of a concrete with a W/C ratio of 0.43 evolves very little between 28 days and 90 days [13], in terms of total porosity, permeability and saturation degree. As there is a clear relationship between porosity and compression strength, these results support once again that the uniaxial compression strength would increase very little for a concrete sample (W/C = 0.63) conserved in water for more than 28 days. Finally, Wood [39] has performed mechanical tests on samples conserved in water for a very long period: he has observed an increase of 11% on compression strength for a concrete with a W/C ratio of 0.71 and 13% for another concrete with a W/C of 0.53, between 28 and 90 days. After 90 days, any variation of strength has not been observed until one year. Such increases should be compared with the increase of 28% obtained in the present study. One can conclude that the increase of strength due to hydration is relatively small after 28 days. Furthermore, the Wood's samples were conserved in water, translating the fact that hydration can be made in an optimal way, without lack of water. Results would have been different if specimens had been only protected from desiccation, because water diffusion towards non-hydrated cement would have been more difficult, and the cement hydration less efficient. Once again, the role of water desiccation on the strength increase is shown.

Finally, in order to compare the elastic property of samples with different moisture contents, under the same stress level, we propose to define the normalised initial modulus, as the initial elastic modulus of each test (determined from the third unloading-reloading cycle) divided by the maximum value among all the compression tests. In the present work, the maximum value is obtained from the specimens dried for 7 days. Fig. 7a and b show the evolution of normalised initial modulus in cylinder specimens as functions of time of drying (Fig. 6a) and loss in mass (Fig. 6b). Each point represents the average value of two tests performed the same day. We

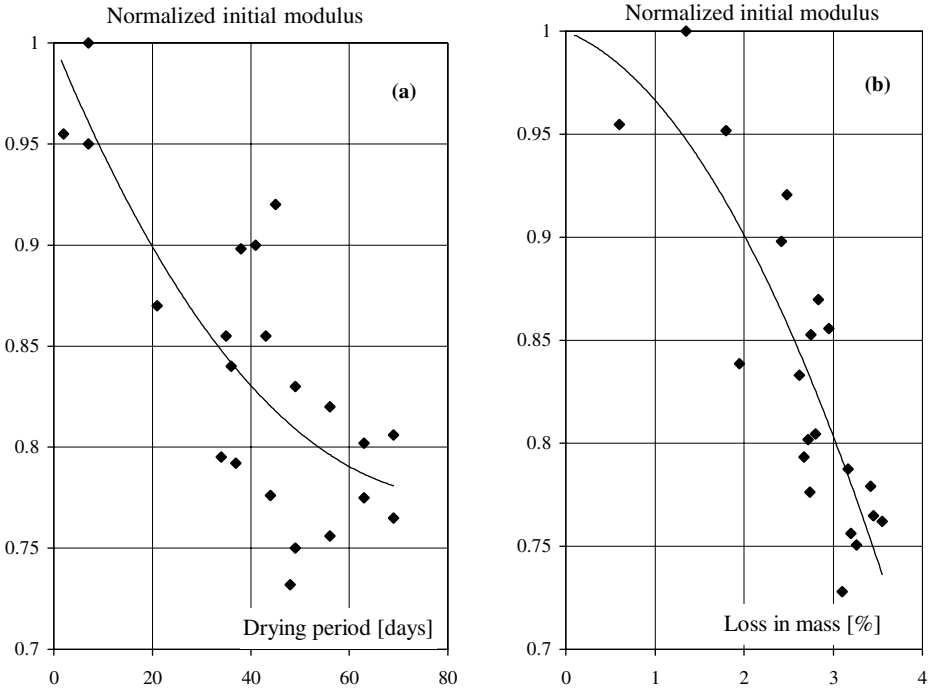

Fig. 7. Evolution of normalised initial stiffness versus time of drying (a) and loss in mass (b).

can see that the normalised initial stiffness regularly decreases during desiccation (about 25%). This means that drying process induces material deterioration by development of microcracks due to local tensile stresses. Similar experimental results have been obtained in uniaxial tension tests [36,40,41]. In the tests conducted by Brooks and Neville [36], such a diminution is of 8% between the elastic modulus respectively measured at 28 and 56 days. In the case of tests performed by Toutlemonde [40], the elastic modulus of a dried concrete is reduced by 32% with respect to a saturated concrete. Concerning the results from Terrien [41], there is a drop in elastic modulus of 12% for a concrete and 30% for a mortar between saturated and dried state. However, drying induced microcracking results in a decrease of 12% in tensile strength, due to the role of this induced initial microcracking on the failure process of specimens. Here it is highlighted that the drying of concrete leads to microcracking because of, on one hand, gradients in drying shrinkage (structural effect due to moisture gradients) and, on the other hand, effect of rigid inclusions (coarse aggregates). These phenomenon also lead to a change of elastic properties of the material, even without mechanical load. There is a decrease in the elastic modulus of concrete. Besides the mechanical behaviour of the material evolves into an elasto-plastic behaviour with softening when it is saturated, towards an elasto-plastic damageable behaviour when its moisture content decreases. This phenomenon can be taken into account by two ways in the modelling: the first is to connect the evolution of the damage variable with the material degree of saturation; the second is to consider the concrete as an elasto-plastic material with damage, partially saturated by water, in which the suction generates plastic contractions, which induce diffused microcracks. It is this second approach which is developed in the second part of this article.

As a preliminary conclusion, this experimental study clearly shows coupled effects between drying process and induced material damage. Mechanical behavior of concrete becomes more brittle in nature with higher damage kinetics when it is dried. There is also material deterioration during proper drying process.

3. Constitutive modelling of partially saturated concrete during drying

In the previous section, we have presented experimental results to show effects of drying shrinkage on mechanical behaviour of concrete. In this section, we propose a constitutive model being able to capture such effects. We have used the elasto-plastic damage model, recently proposed by the authors [42], for concrete in partially saturated conditions. We present here the essential features of the model. The formulation of the model is based on the mechanics of porous media initiated by Biot. The concrete is assumed to be saturated by a liquid phase (noted by index 'w') and a gas mixture (noted by index 'g'). The gas mixture is a perfect mixture of dry air (noted by index 'da') and vapour (noted by index 'va'). We assume an isotropic behaviour of concrete and consider isothermal evolutions only. By adopting the assumption of small strains, the total strain tensor is decomposed into an elastic part and plastic part:

$$\varepsilon_{ij} = \varepsilon^{e}_{ij} + \varepsilon^{p}_{ij}, \quad d\varepsilon_{ij} = d\varepsilon^{e}_{ij} + d\varepsilon^{p}_{ij} \tag{1}$$

The basic poroelastic behaviour of concrete is described by using the non-linear poroelastic model proposed by Coussy [43,44]. The incremental form of constitutive equations is expressed as follows:

$$d\sigma_{ij} = C^{0}_{ijkl} d\varepsilon^{e}_{kl} - b[S_w dp_w + (1 - S_w) dp_g]\delta_{ij} \tag{2}$$

$$\begin{aligned} dp_g &= dp_{va} + dp_{da} \\ &= \frac{p_g}{\phi_g}\left[-b d\varepsilon^{e}_{v} + \left(\frac{dm}{\rho}\right)^{e}_{w}\right] + \frac{p_{va}}{\phi_g}\left(\frac{dm}{\rho}\right)^{e}_{va} + \frac{p_{da}}{\phi_g}\left(\frac{dm}{\rho}\right)^{e}_{da} \end{aligned} \tag{3}$$

$$dp_c = dp_g - dp_w = -M_c\left[-bS_w d\varepsilon^{e}_{v} + \left(\frac{dm}{\rho}\right)^{e}_{w}\right] \tag{4}$$

where σ_{ij} are the components of stress tensor, the fourth order tensor $\widetilde{C}^{0}$ is the initial elastic stiffness of undamaged material, ε^{e}_{ij} are the components of elastic strain tensor, and ε^{e}_{v} the elastic volumetric strain. The parameter b denotes Biot's coefficient of porous medium and S_w the water saturation degree, and ϕ_g the porosity occupied by gas mixture. The scalar variable $(\frac{dm}{\rho})^{e}_{k}$ represents the elastic variation of mass of the kth fluid phase per unit initial volume of porous medium, and p_k the pressure of the kth fluid phase. In Eq. (4), the variable p_c defines the capillary pressure. The parameter M_c is Biot's modulus related to capillary pressure, which is a function of water saturation degree:

$$M_c = -\frac{1}{\phi_0 + \varepsilon_v}\left(\frac{dp_c}{dS_w}\right), \quad p_c = p_g - p_w \tag{5}$$

where ϕ_0 is the initial porosity and ε_v the volumetric strain.

The emphasis of modelling is on the description of coupled plastic damage due to drying shrinkage. The formulation of plasticity is simplified: we have used the classic Drücker-Prager criterion for the yield function. A non-associated flow rule has been used through a linear plastic potential [42]. In order to take into account the effects of capillary pressure and induced damage on plastic behaviour of concrete, we proposed an extension of the Bishop effective stress concept [45] to plastic flow of unsaturated concrete with isotropic damage. The following modified effective stress tensor has been used:

$$\hat{\sigma} = \frac{\sigma + \beta[p_g - S_w p_c]\mathbf{I}}{1-d} \tag{6}$$

The parameter β, different from Biot's coefficient b, defines the dependency of plastic behaviour upon the variation of saturation condition. The scalar variable d describes the isotropic damage of material.

The induced damage affects elastic properties of material. In the case of isotropic damage, we assume that only the elastic modulus is decreasing due to material damage. Therefore, the elasto-plastic constitutive equation (2) is completed by including the variation of elastic stiffness due to material damage:

$$\mathrm{d}\sigma_{ij} = (1-d)\cdot C^0_{ijkl}\mathrm{d}\varepsilon^e_{kl} - \mathrm{d}(d)\cdot C^0_{ijkl}\varepsilon^e_{kl} - b[S_w \mathrm{d}p_w + (1-S_w)\mathrm{d}p_g]\delta_{ij} \tag{7}$$

The characterisation of damage evolution is based on the model proposed by Mazars [8]. However, we have adapted the damage criterion (f_d) to include the contribution of plastic strain to damage evolution:

$$f_d = \tilde{\varepsilon} - k(d) \leqslant 0,$$
$$\tilde{\varepsilon} = \tilde{\varepsilon}^e + \tilde{\varepsilon}^p = \sqrt{\sum_i (\varepsilon_i^{e+})^2} + \sqrt{\sum_i (\varepsilon_i^{p+})^2} \tag{8}$$

where $\tilde{\varepsilon}$ is the equivalent strain, $k(d)$ is the damage threshold, ε_i^{e+} and ε_i^{p+} are the elastic and plastic principal tensile strain. As in the initial model of Mazars, the total damage is a linear combination of those respectively induced by the tensile stress (d_t) and compressive stress (d_c):

$$d = \alpha_t d_t + (1-\alpha_t) d_c \tag{9}$$

The coefficient α_t defines the ratio between two parts of the damage [8,42]. The evolution of each damage component is respectively determined by the following equations [8]:

$$d_t = 1 - \frac{\varepsilon_{d0}(1-A_t)}{\varepsilon_M} - \frac{A_t}{\exp[B_t(\varepsilon_M - \varepsilon_{d0})]} \tag{10}$$

$$d_c = 1 - \frac{\varepsilon_{d0}(1-A_c)}{\varepsilon_M} - \frac{A_c}{\exp[B_c(\varepsilon_M - \varepsilon_{d0})]} \tag{11}$$

where the parameter ε_{d0} is the initial damage threshold while ε_M represents the maximum value reached by the equivalent strain $\tilde{\varepsilon}$ during the loading history (current damage threshold). Four parameters A_c, B_c, A_t and B_t control damage evolution rate under tensile and compressive stresses.

The parameters involved in the constitutive model can be determined from experimental data obtained in uniaxial and triaxial compression tests (see details in [42]), and the set of material parameters presented in Table 2 has been used for the next numerical simulations. By using the proposed model, we have simulated some basic mechanical tests. In Fig. 8, we present the comparison between experimental data and numerical simulation for a representative uniaxial compression test (saturated case). We can see the capacity of model to reproduce basic mechanical properties of concrete, in particular, plastic strains and deterioration of elastic properties due to damage. In Fig. 9, we compare numerical simulations between uniaxial compression and tension test in saturated case ($S_w = 100\%$). The asymmetric response of concrete in tension and compression is well described. In order to reproduce the effects of

Table 2
Material parameters used in the simulations

Elastic parameters	*Plastic parameters*
$E = 27000$ MPa	$\beta = 0.084$
$\nu = 0.2$	$\alpha_0 = 0.0$
Damage parameters	$\alpha_r = 1.55$
$\varepsilon_{d0} = 1\times10^{-4}$	$\chi = 2800$
$A_t = 1$	$C_0 = 1.27$ MPa
$B_t = 5000$	$\eta = 0.2$
$A_c = 0.967$	$s_0^d = 23$ MPa
$B_c = 108.56$	$h = -1000$

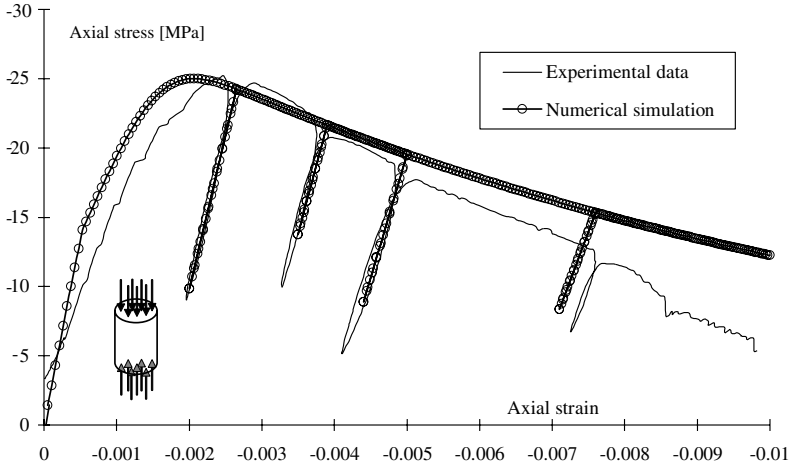

Fig. 8. Comparison between simulation and test data in an uniaxial compression test with unloading phase (continuous lines are test results) for a saturated concrete.

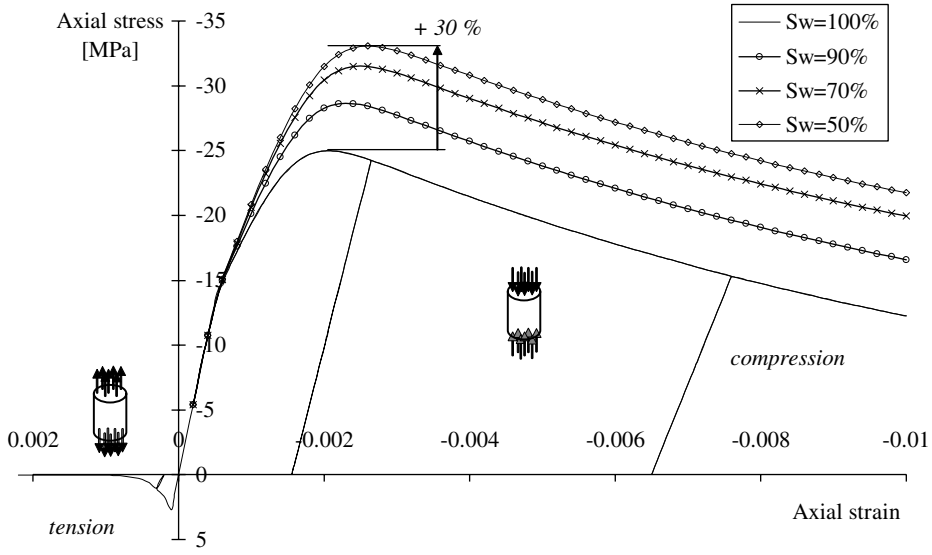

Fig. 9. Numerical predictions of concrete response in uniaxial tension and compression test and influences of water saturation degree on compressive behaviour.

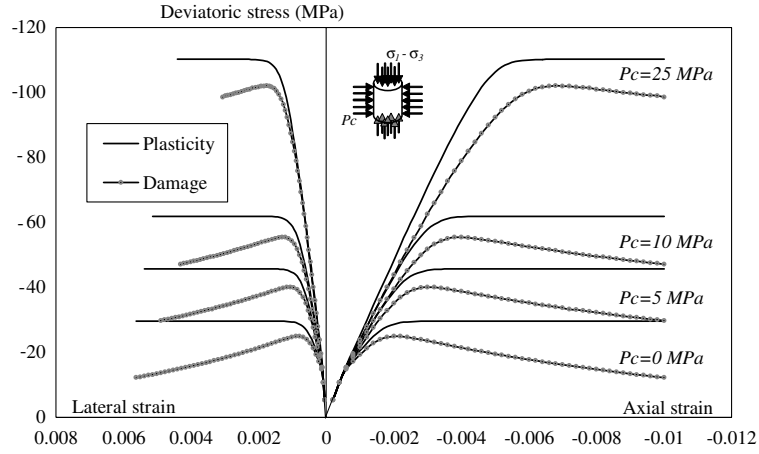

Fig. 10. Numerical simulations of triaxial compression tests with different confining pressure: plasticity approach and coupled damage-plasticity calculations.

water saturation degree on the mechanical properties of concrete, we have to determine the water retention curve, which relates the suction to water saturation degree. Based on the results reported in literature, the following equation is used:

$$S_w = [1 + (ap_c)^b]^c, \quad a = 2.35 \times 10^{-8}$$
$$b = 1.83, \quad c = -0.58 \tag{12}$$

In Fig. 9, we show simulations of four homogeneous uniaxial compression tests with different degree of water saturation. Increase in uniaxial compression strength (about 30% in numerical simulation) is well reproduced by the proposed model.

In Fig. 10, we show numerical simulations of four triaxial compression tests with different confining pressure. Even if these results are not compared with experimental data for the concrete tested here, they are qualitatively in good accordance with most data obtained from classic concrete. Material behaviour becomes more ductile when confining pressure increases. On this figure, we also compare the simulations obtained with the elasto-plastic model without damage, and those with coupled elastic-plastic damage. We can see the important contribution of damage on overall behaviour of concrete.

4. Simulation of drying process in a concrete cylinder

In this section, we present simulations of the drying tests presented in Section 2. As mentioned before, during these tests, the water saturation degree (then stresses and strains) is not uniform inside samples. We have to

solve a boundary values problem for numerical simulation of drying tests. Therefore, the proposed model is implemented in a FEM code (named MPPSAT), which is devoted to hydromechanical problems of partially saturated media. A fully coupled algorithm is used. The governing equations have been presented in [42]. The basic data used for the simulations are the variation of relative permeability for liquid and gas. In this work, we have used the following equations from [18], for a classic concrete:

$$k_l^r = \sqrt{S_w}[1 - (1 - S_w^{1/a})^a]^2, \quad a = 0.17 \tag{13}$$

$$k_g^r = \sqrt{1 - S_w}[1 - S_w^{1/a}]^{2a} \tag{14}$$

The drying process of cylinder is analysed in axisymmetric conditions. The cylinder is assumed initially saturated. Due to symmetry, only a quarter of a cylinder is considered (h = 110 mm, l = 55 mm). The mesh is composed of 400 eight-node quadratic elements. The values of the used material parameters are given in Table 2. It is submitted to drying on the right lateral surface with a relative humidity of H_r = 60% while no flow conditions are prescribed on the left lateral, top and bottom surfaces. The numerical model predicts a too fast drying kinetics [42], because possible variation of permeability due to damage is not taking into account in the present simulation. Indeed, we should point out that numerical results are obtained by calculating average value of water saturation in sample volume, and numerical simulations are strongly sensitive to input data, such as evolution of relative permeability of water.

In Fig. 11, we compare model's predictions and experimental data on the evolution of uniaxial compression strength as a function of drying time (or equivalently

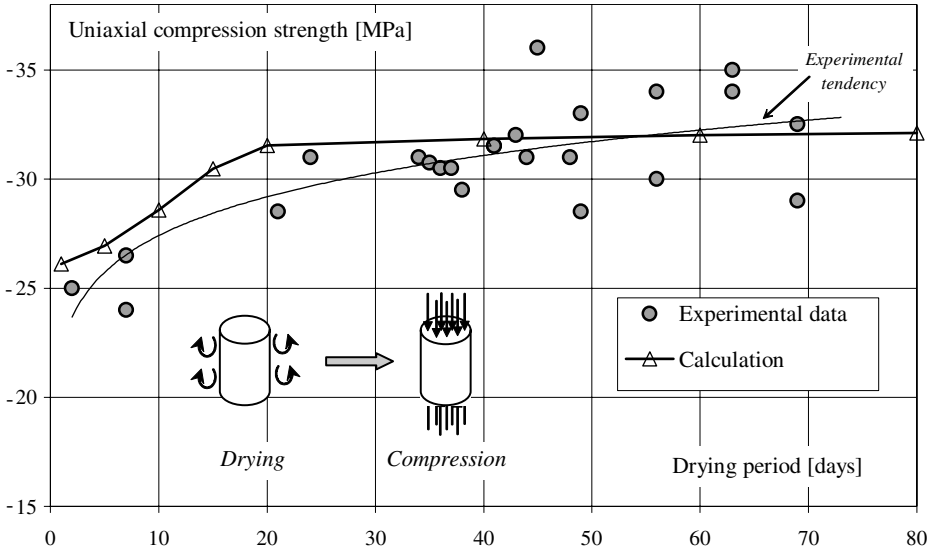

Fig. 11. Evolution of uniaxial compression strength as a function of drying time: comparison between simulations and test data.

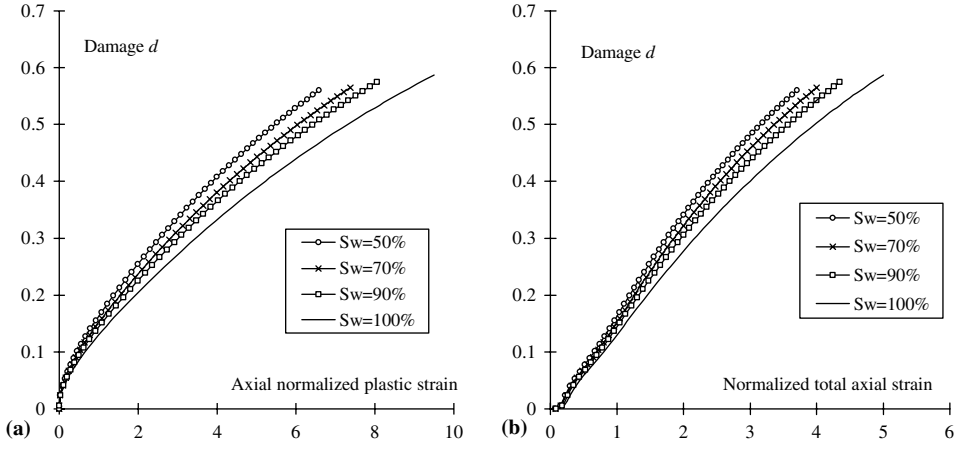

Fig. 12. Evolution of induced damage as a function of normalized plastic strain (a) and normalized total axial strain (b) in uniaxial compression test with different water saturation degree: numerical predictions.

water saturation degree). Once again, we obtain a good agreement from the qualitative and quantitative points of view, also with most data found in the literature (for example [29–36]). In Fig. 12a and b, we show simulations of four homogeneous uniaxial compression tests with different degree of water saturation (average value on each sample). We present evolutions of damage variable as a function of normalised irreversible axial strain (Fig. 12a) and normalised total axial strain (Fig. 12b). We can notice that damage kinetics is higher in samples with lower saturation degree. This means that the compression strength of concrete increases with drying but the material becomes more brittle. Such a result is qualitatively confirmed by experimental data shown in Fig. 5a and b.

5. Concluding remarks

A preliminary experimental investigation has been performed in order to study effects of drying shrinkage on mechanical behaviour of concrete. Uniaxial compression tests have been conducted on samples submitted to different periods of drying. The obtained results have clearly shown coupled phenomena between drying process and material damage. Uniaxial compression strength increases with desiccation due to developed capillary forces. Material behaviour becomes more brittle and therefore is reflective of a higher damage kinetics when concrete is progressively dried. There is also material damage during proper drying process. Thus, two competition effects appear during drying of cementitious materials: the effect of capillary suction increasing the mechanical strength of material, and the degradation of elastic properties by induced microcracks. A simple elasto-plastic damage model is then proposed for modelling of hydro-mechanical behaviour of partially saturated concrete. Even if only isotropic behaviour is concerned, the model is able to describe principal responses of concrete under mechanical and hydrous conditions. Let us note that this model, to be used in a more practical way, can be easily coupled with concrete maturation models (for example [46,47]). Numerical simulations of uniaxial compression tests are in qualitative agreement with experimental data. The obtained results have clearly shown that it is important to take into account effects of drying in analysis of strength and failure in concrete structures.

References

[1] Acker P. Comportement mécanique du béton: apports de l'approche physico-chimique. Phd Thesis of Ecole Nationale des Ponts et Chaussées, Paris, Rapport de Recherche LPC 152, 1988 [in French].
[2] Bažant ZP, Wittmann FH, editors. Creep and shrinkage in concrete structures. London: John Wiley; 1982.
[3] Wittmann FH. Deformation of concrete at variable moisture content. In: Bažant ZP, editor. Mechanics of geomaterials. London: John Wiley; 1985.
[4] Baroghel-Bouny V, Aïtcin P-C, editors. Shrinkage of Concrete, Proc of Int RILEM Workshop Shrinkage 2000, RILEM Publications PRO 17, Paris, France, 2000.
[5] Reinhardt HW. Relation between the microstructure and structural performance of concrete. In: Aguado A, Gettu R, Shah S, editors. Proceedings of the Int RILEM Workshop on Technology Transfer on the New Trend in Concrete, ConTech'94, Barcelona, 1994, p. 19–32.
[6] Wittmann FH. Creep and shrinkage mechanisms. In: Bažant ZP, Wittmann FH, editors. Creep and shrinkage in concrete structures. London: John Wiley; 1982. p. 129–61.
[7] Bažant ZP, Raftshol WJ. Effect of cracking in drying and shrinkage specimens. Cem Concr Res 1982;12:209–26.
[8] Mazars J. Application de la mécanique de l'endommagement au comportement non linéaire et á la rupture du béton de structure. Thèse de Doctorat d'Etat de l'Université Paris 6, 1984 [in French].
[9] Aïtcin P-C, Neville A, Acker P. Integrated view of shrinkage deformation. Concr Int 1997;19(9):35–41.
[10] Bažant ZP. Criteria for rational prediction of creep and shrinkage of concrete. Rev Fr Génie Civ 1999;3(3–4):61–89.
[11] Ulm FJ, Le Maou F, Boulay C. Creep and shrinkage coupling: new review of some evidences. Rev Fr Génie Civ 1999; 3(3–4):21–37.
[12] Baroghel-Bouny V. Caractérisation microstructurale et hydrique des pâtes de ciment et des bétons ordinaires et à très hautes performances. PhD thesis of Ecole Nationale des Ponts et Chaussées, Paris, 1994 [in French].
[13] Baroghel-Bouny V, Rougeau P, Care S, Gawsewitch J. Etude comparative de la durabilitédes bétons B30 et B80. I—Microstructure, propriétés de durabilitéet retrait. Bull Liaison Lab Ponts Chaussées 1998;217:61–73 [in French].
[14] de Larrard F, Le Roy R. Relation entre formulation et quelques propriétés mécaniques des bétons à hautes performances. Mater Struct 1992;25:464–75 [in French].
[15] Hearn N. Effect of shrinkage and load-induced cracking on water permeability of concrete. ACI Mater J 1999;96:234–41.
[16] Bisschop J, Pel L, van Mier JGM. Effect of aggregate size and paste volume on drying shrinkage microcracking in cement-based composites. In: Ulm F-J, Bažant ZP, Wittmann FH, editors. Creep, shrinkage & durability mechanics of concrete and other quasi-brittle materials. Amsterdam: Elsevier; 2001. p. 75–80.
[17] Bisschop J, van Mier JGM. How to study drying shrinkage microcracking in cement-based materials using optical and scanning electron microscopy?. Cem Concr Res 2002;32(2):279–87.
[18] Mainguy M, Coussy O, Baroghel-Bouny V. Role of air pressure in drying of weakly permeable materials. ASCE J Engrg Mech 2001;127(6):582–92.
[19] Samaha HR, Hover KC. Influence of microcracking on the mass transport properties of concrete. ACI Mater J 1992;89(4):416–24.
[20] Pihlajavaara SE. Estimation of drying of concrete at different relative humidities and temperatures of ambient air with special discussion about fundamental features of drying and shrinkage. In: Bažant ZP, Wittmann FH, editors. Creep and shrinkage in concrete structures. London: John Wiley; 1982. p. 87–108.
[21] Granger L, Torrenti JM, Diruy M. Simulation numérique du retrait du béton sous hygrométrie variable. Bull Liaison Lab Ponts Chaussées 1994;190:57–64 [in French].
[22] Colina H, Acker P. Drying cracks: kinematics and scale laws. Mater Struct 2000;33:101–7.
[23] Huet C, Acker P, Baron J. Fluage et autres effets rhéologiques différées du béton, in: Le béton hydraulique. Presse de l'Ecole Nationale des Pont et Chaussées, Paris, 1982 [in French].
[24] Neville AM. Properties of concrete. 4th ed. Longman Group; 1995.

[25] Meftah F, Torrenti JM, Nechnech W, Bendoudjema F, de Sa C. An elasto -plastic damage approach for the modelling of concrete submitted to the mechanical induced effects of drying. In: Baroghel-Bouny V, Aïtcin P-C, editors. Shrinkage of Concrete, Proc of Int RILEM Workshop Shrinkage 2000, RILEM Publications PRO 17, Paris, France, 2000, p. 341–54.
[26] Bažant ZP, Sener S, Kim JK. Effect of cracking on drying permeability and diffusivity of concrete. ACI Mater 1986; 84(31–32):351–7.
[27] Meziani H, Skoczylas F. An experimental study of the mechanical behaviour of a mortar and its permeability under deviatoric loading. Mater Struct 1999;32:403–9.
[28] Pihlajavaara SE. A review of some of the main results of a research on the ageing phenomena of concrete, effect of moisture conditions on strength, shrinkage and creep of mature concrete. Cem Concr Res 1974;4:761–71.
[29] Popovics S. Effect of curing method and final moisture condition on compressive strength of concrete. ACI J 1986;83:650–7.
[30] Bartlett FM, MacGregor JG. Effect of moisture condition on concrete core strengths. ACI Mater J 1993;91(3):227–36.
[31] Yaman IO, Hearn N, Aktan HM. Active and non-active porosity in concrete; Part I: Experimental evidence. Mater Struct 2002;35:102–9.
[32] Lange DA. Strength development of pavement concretes. ASCE J Mater Civil Engrg 1994;6(1):78–87.
[33] Al-Khaiat H, Fattuhi N. Long-term strength development of concrete in arid conditions. Cem Concr Comp 2001;23(4–5): 363–73.
[34] Dantec P, Terme G. Séchage et comportement différé du béton: influence de la cinétique de dessiccation sur le comportement des bétons, LCPC report no. 1.41.02.5, Paris, 1996 [in French].
[35] Okajima T, Ishikawa T, Ichise K. Moisture effect on the mechanical properties of cement mortare. Trans Jpn Concr Inst 1980;2:125–32.
[36] Brooks JJ, Neville AM. A comparison of creep, elasticity, and strength of concrete in tension and in compression. Mag Concr Res 1977;29:131–41.
[37] Torrenti J-M. Comportement multiaxial du béton: Aspects expérimentaux et modélisation. Phd thesis of Ecole Nationale des Ponts et Chaussées, Paris, 1987 [in French].
[38] Yurtdas I, Burlion N, Skoczylas F. Experimental characterisation of the drying effect on uniaxial mechanical behaviour of mortar. Mater Struct 2004;37:170–6.
[39] Wood SL. Evaluation of the long-term properties of concrete. ACI Mater J 1991;88(6):630–43.
[40] Toutlemonde F. Résistance au choc des structures en béton. Phd thesis of Ecole Nationale des Ponts et Chaussées, Paris, 1994 [in French].
[41] Terrien M. Emission acoustique et comportement mécanique post-critique d'un béton sollicité en traction. Bull Liaison Lab Ponts Chaussées 1980;105:65–72 [in French].
[42] Bourgeois F, Burlion N, Shao JF. Modelling of elastoplastic damage in concrete due to desiccation shrinkage. Int J Numer Anal Methods Geomech 2002;26:759–74.
[43] Coussy O. Mechanics of porous continua. New York: John Wiley; 1995.
[44] Coussy O, Eymard R, Lassabatère T. Constitutive modelling of unsaturated drying deformable materials. ASCE J Engrg Mech 1998;124(6):658–67.
[45] Bishop AW, Blight GE. Some aspects of effective stress in saturated and partly saturated soils. Géotechnique 1963; 13(3):177–97.
[46] Ulm F-J, Coussy O. Couplings in early-age concrete: from material modelling to structural design. Int J Solid Struct 1998;35(31–32):4295–311.
[47] Ulm F-J, Coussy O. Strength growth as chemo-plastic hardening in early age concrete. ASCE J Engrg Mech 1996;122(12):1123–32.